Fast Collisionless Reconnection and Electron Heating in Strongly Magnetized Plasmas

N. F. Loureiro,[1] A. A. Schekochihin,[2] and A. Zocco[3,2]

[1]*Associação EURATOM/IST, Instituto de Plasmas e Fusão Nuclear—Laboratório Associado, Instituto Superior Técnico, Universidade Técnica de Lisboa, 1049-001 Lisboa, Portugal*

[2]*Rudolf Peierls Centre for Theoretical Physics, University of Oxford, Oxford OX1 3NP, United Kingdom*

[3]*EURATOM/CCFE Fusion Association, Culham Science Centre, Abingdon OX14 3DB, United Kingdom*

(Received 2 January 2013; published 10 July 2013)

Magnetic reconnection in strongly magnetized (low-beta), weakly collisional plasmas is investigated by using a novel fluid-kinetic model [Zocco and Schekochihin, Phys. Plasmas **18**, 102309 (2011)] which retains nonisothermal electron kinetics. It is shown that electron heating via Landau damping (linear phase mixing) is the dominant dissipation mechanism. In time, electron heating occurs after the peak of the reconnection rate; in space, it is concentrated along the separatrices of the magnetic island. For sufficiently large systems, the peak reconnection rate is $cE_{\parallel}^{\max} \approx 0.2 v_A B_{y,0}$, where v_A is the Alfvén speed based on the reconnecting field $B_{y,0}$. The island saturation width is the same as in magnetohydrodynamics models except for small systems, when it becomes comparable to the kinetic scales.

DOI: 10.1103/PhysRevLett.111.025002 PACS numbers: 52.35.Vd, 52.30.Gz, 52.35.Py, 96.60.Iv

Introduction.—Magnetic reconnection is a reconfiguration of the magnetic field in a plasma via localized unfreezing of the magnetic flux [1]. It is commonly associated with energy release in astrophysical and laboratory plasmas, but the details of the energy conversion mechanisms and partition between particle species and fields are poorly understood. This Letter focuses on a key aspect of this issue: the conversion of the magnetic energy into electron internal energy, i.e., electron heating.

We consider a fundamental reconnection paradigm: the tearing mode in a periodic box [2]. The tearing instability leads to the opening, growth, and saturation of a magnetic island [2–6]. If the saturated island is macroscopic, it must be a magnetohydrodynamics (MHD) solution; i.e., it cannot depend on the microphysics of the plasma (e.g., on collisionality). We will confirm this and show that the final state is unique. This implies that the total fraction of the initial magnetic energy converted to other forms of energy from the beginning to the end of the evolution of the tearing mode must be independent of collisionality. In a periodic (closed) system, energy cannot be lost via bulk plasma outflows. Therefore, the magnetic energy difference between the initial and final states must be accounted for by conversion into the thermal energy of the particles. In collisional plasmas, this is achieved by Ohmic and viscous heating [7]. However, many natural systems where reconnection occurs are only weakly collisional; the only available heating channels then are Landau damping and electron viscosity, both of which ultimately rely on the electron collision frequency being finite, though possibly arbitrarily small. In this Letter, we show that electron heating via linear phase mixing associated with Landau damping is the main energy conversion channel in weakly collisional reconnection in strongly magnetized (low-beta) plasmas.

Equations.—We use a fluid-kinetic model applicable to low-beta plasmas ("KREHM" [8]). One of its features is the coupling of Ohm's law to the electron (drift) kinetic equation via the electron temperature fluctuations $\delta T_{\parallel e}$. The kinetic equation supports collisions, Landau resonance, and phase mixing, thus enabling kinetic electron heating mechanisms accompanied by entropy production.

We work in the low-β regime, where β, the ratio of the plasma to the magnetic pressure, is ordered similar to the electron-ion mass ratio m_e/m_i. The perturbed electron distribution function, to lowest order in $\sqrt{m_e/m_i} \sim \sqrt{\beta}$, and in the gyrokinetic expansion [9–12], is defined as $\delta f_e = g_e + (\delta n_e/n_{0e} + 2v_\parallel u_{\parallel e}/v_{\mathrm{the}}^2)F_{0e}$, where F_{0e} is the equilibrium Maxwellian, $v_{\mathrm{the}} = \sqrt{2T_{0e}/m_e}$ is the electron thermal speed (with T_{0e} the mean electron temperature), $v_\parallel$ is the parallel velocity coordinate, $\delta n_e/n_{0e}$ is the electron density perturbation (the zeroth moment of δf_e) normalized to its background value n_{0e}, and $u_{\parallel e} = (e/cm_e)d_e^2\nabla_\perp^2 A_\parallel$ is the parallel electron flow (the first moment of δf_e; $A_\parallel$ is the parallel component of the vector potential, and $d_e = c/\omega_{pe}$ is the electron skin depth). All moments of δf_e higher than δn_e and $u_{\parallel e}$ are contained in g_e, e.g., $\delta T_{\parallel e}/T_{0e} = (1/n_{0e})\int d^3\mathbf{v}(2v_\parallel^2/v_{\mathrm{the}}^2)g_e$. In the 2D case considered here, the dynamics of the plasma is described by the following equations [8]:

$$\frac{1}{n_{0e}}\frac{d\delta n_e}{dt} = \frac{1}{B_z}\left\{A_\parallel, \frac{e}{cm_e}d_e^2\nabla_\perp^2 A_\parallel\right\}, \tag{1}$$

$$\frac{d}{dt}(A_\parallel - d_e^2\nabla_\perp^2 A_\parallel) = -\frac{cT_{0e}}{eB_z}\left\{A_\parallel, \frac{\delta n_e}{n_{0e}} + \frac{\delta T_{\parallel e}}{T_{0e}}\right\}, \tag{2}$$

$$\frac{dg_e}{dt} - \frac{v_\parallel}{B_z}\left\{A_\parallel, g_e - \frac{\delta T_{\parallel e}}{T_{0e}}F_{0e}\right\} = C[g_e] - \left(1 - \frac{2v_\parallel^2}{v_{\mathrm{the}}^2}\right)\frac{F_{0e}}{B_z}\left\{A_\parallel, \frac{e}{cm_e}d_e^2\nabla_\perp^2 A_\parallel\right\}, \tag{3}$$

where $C[g_e]$ is the collision operator, $\{\ldots,\ldots\}$ is the Poisson bracket, and $d/dt = \partial/\partial t + c/B_z\{\varphi,\ldots\}$, with B_z the out-of-plane magnetic guide field and φ the electrostatic potential. The latter is obtained via $\delta n_e/n_{0e} = 1/\tau(\hat{\Gamma}_0 - 1)e\varphi/T_{0e}$ [10], where $\tau = T_{0i}/T_{0e}$ and $\hat{\Gamma}_0$ denotes the inverse Fourier transform of $\Gamma_0(\alpha) = I_0(\alpha)e^{-\alpha}$, with I_0 the modified Bessel function and $\alpha = k_\perp^2\rho_i^2/2$ ($\rho_i = v_{\mathrm{th}i}/\Omega_i$ is the ion Larmor radius).

Equation (3) shows that the isothermal closure [13] $g_e = 0$ is not a solution of that equation unless $\{A_\parallel, \nabla_\perp^2 A_\parallel\} = 0$, a condition that cannot describe a reconnecting system [though it does describe the (macroscopic) island saturation [4,5], as we will find]. Therefore, the possibility of electron heating in our system cannot be ignored.

Numerical details.—Equation (3) does not contain an explicit dependence on the perpendicular velocity coordinate $v_\perp$. If we ignore any such dependence that is introduced by the collision operator, $v_\perp$ can be integrated out, so $g_e = g_e(x, y, v_\parallel, t)$. Next, we introduce the Hermite expansion $g_e(x, y, v_\parallel, t) = \sum_{m=2}^{\infty} H_m(v_\parallel/v_{\mathrm{th}e})g_m(x, y, t)F_{0e}(v_\parallel)/\sqrt{2^m m!}$ ($g_0 = g_1 = 0$, because δn_e and $u_{\parallel e}$ have been explicitly separated in the decomposition of δf_e adopted above). Equation (3) then unfolds into a series of coupled, fluidlike equations for each of the coefficients g_m:

$$\frac{dg_m}{dt} = \frac{v_{\mathrm{th}e}}{B_z}\left(\sqrt{\frac{m+1}{2}}\{A_\parallel, g_{m+1}\} + \sqrt{\frac{m}{2}}\{A_\parallel, g_{m-1}\}\right) + \frac{\sqrt{2}}{B_z}\delta_{m,2}\left\{A_\parallel, \frac{e}{cm_e}d_e^2\nabla_\perp^2 A_\parallel\right\} - \nu_{\mathrm{coll}}(m^4 g_m - 16\delta_{m,2}g_2), \quad (4)$$

where we have adopted a model (hyper)collision operator with $\nu_{\mathrm{coll}} = 1/(\Delta t M^4)$, where M is the index of the highest Hermite polynomial kept in a simulation and Δt the time step. Thus, in our simulations, M is a proxy for the collision frequency, with higher values of M corresponding to less collisional systems (at the large values of M reported here, $\Delta t \propto M^{-1/2}$, so $\nu_{\mathrm{coll}} \propto M^{-7/2}$).

Equations (1), (2), and (4) are solved numerically by using a pseudospectral code [14]. The spatial grid size is 384^2. The resolution in velocity space is set by M and ranges from 30 to 500. Hyperdiffusive terms of the form $\nu_H\nabla_\perp^6$, where $\nu_H = 0.25/\Delta t(\Delta x/\pi)^6$, with Δx the grid spacing, are added to the right-hand side of Eq. (1) (electron hyperviscosity), Eq. (2) (hyper-resistivity), and Eq. (4). These are required to prevent the nonlinear unbounded thinning of the current layer [15–17] but will not, as we will discover, dissipate much energy [18]. In the following, "hyperdissipation" refers to the hyperdiffusive terms in all equations; "Landau" is the dissipation due to hypercollisions in Eq. (4), accessed via phase mixing (which moves energy to higher m). These are the only two dissipation mechanisms present in our simulations.

The equilibrium in-plane magnetic field (asymptotically smaller than the guide field B_z) is $B_{y,\mathrm{eq}} = -dA_{\parallel\mathrm{eq}}/dx$, with $A_{\parallel\mathrm{eq}} = A_{\parallel 0}/\cosh^2(x/a)$, where a is the (normalizing) equilibrium scale length. The (normalizing) Alfvén time is defined as $\tau_A = a/v_A$ with v_A the Alfvén speed based on $B_{y,0} = \max|B_{y,\mathrm{eq}}| = 1$. The simulations are performed in a doubly periodic box of dimensions $L_x \times L_y$, with $L_x/a = 2\pi$ and L_y such that $\hat{k}_y = 2\pi a/L_y$ yields the desired value of the tearing instability parameter $\Delta' a = 2(5 - \hat{k}_y^2) \times (3 + \hat{k}_y^2)/(\hat{k}_y^2\sqrt{4 + \hat{k}_y^2})$ [6]. For simplicity and numerical convenience, we set $\rho_i = \rho_s = d_e = 0.25a$, where $\rho_s = \rho_i/\sqrt{2\tau}$.

Reconnection rate.—The time traces of the reconnection rate, defined as the value of the parallel electric field at $(x, y) = (0, 0)$ (the X point), $E_\parallel$, are plotted in Fig. 1(a). As shown, the reconnection rate is entirely independent of collisionality (parameterized by M), consistent with the fact that our simulations are in the weakly collisional regime, where the frozen-flux constraint is broken by electron inertia, not the collisions. The maximum value is $cE_\parallel^{\max} \approx 0.22 v_A B_{y,0}$, similar to the fast reconnection rates obtained in the opposite limit of weak guide field [19] and in qualitative agreement with Refs. [20,21]. Regarding the dependence of $E_\parallel^{\max}$ with system size (not shown), we found that $E_\parallel^{\max}$ increases with Δ', asymptoting to $cE_\parallel^{\max} \sim 0.2 v_A B_{y,0}$ for $\Delta' a \gtrsim 10$.

Figure 2 depicts the system configuration for our least collisional simulation ($M = 500$, i.e., $\nu_{\mathrm{coll}}\tau_A \sim 2 \times 10^{-7}$) at the time of maximum reconnection rate [$t/\tau_A = 22.7$; see Fig. 1(a)] (top row) and at the time of maximum dissipation rate [$t/\tau_A = 29.4$; see Fig. 1(b)] (bottom row).

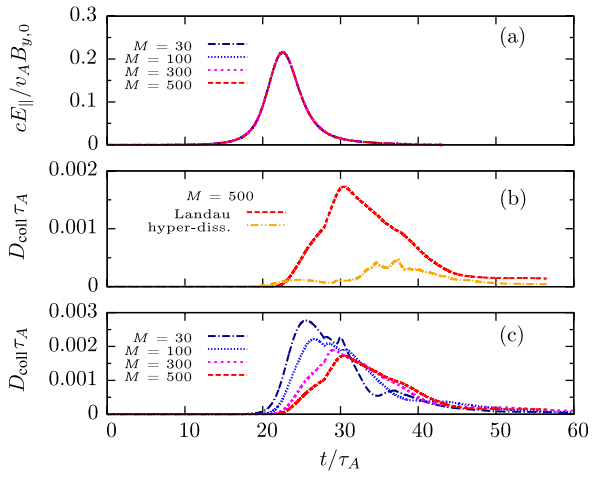

FIG. 1 (color online). Time traces of (a) the reconnection rate for different values of collisionality (represented by M; larger M means less collisions); (b) the rates of dissipation via Landau damping and hyperdissipation, for the least collisional case ($M = 500$); (c) the rate of dissipation via Landau damping for different values of M. All runs had $\Delta' a = 20$.

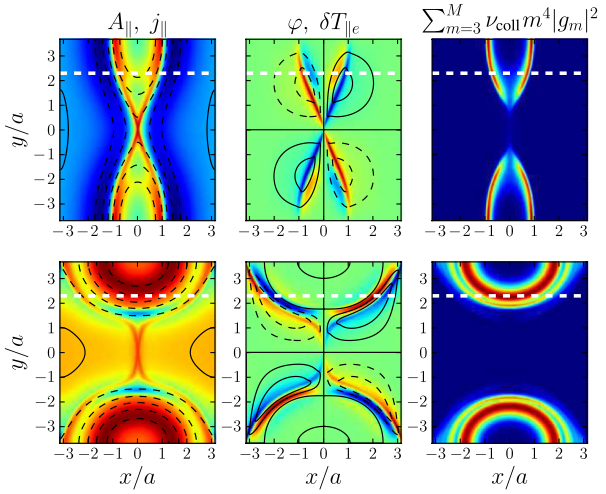

FIG. 2 (color online). System configuration for our least collisional simulation ($M = 500$) at the time of maximum reconnection rate (top row) and of maximum dissipation rate (bottom row). Shown are $A_\parallel$ [lines: full (dashed) are positive (negative) contours] and $j_\parallel = -c/4\pi\nabla_\perp^2 A_\parallel$ [colors: the color scale is linear, ranging from blue to red; units are arbitrary]; φ (lines) and $\delta T_{\parallel e}$ (colors); the collisional dissipation via g_m's (i.e., via Landau damping). The horizontal dashed line marks the location of the domain cut where the distribution function of Fig. 4 (bottom row) is plotted.

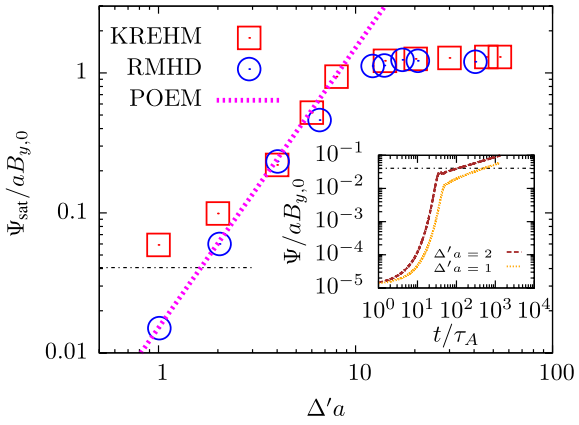

FIG. 3 (color online). Saturated flux $\Psi_{\rm sat}$ vs Δ'. KREHM are the data from the kinetic simulations; RMHD are MHD results from Ref. [6]. The dotted line (POEM) is the prediction from MHD theory [4,5]. Inset: Time traces of flux for $\Delta' a = (1, 2)$. In both plots, the horizontal line is the saturated flux corresponding to a full island width of $2d_e/a$.

A typical X-point geometry is seen, accompanied by a quadrupole structure in $\delta T_{\parallel e}$ (and in δn_e, not shown) [22].

Saturation.—Figure 3 shows the saturation amplitudes obtained in our simulations ("KREHM"); overplotted are the MHD ($\rho_{s,i} = d_e = 0$) results from Ref. [6] ("RMHD"). "POEM" is the prediction from MHD theory [4,5], valid in the small-$\Delta' a$ regime. As anticipated, we find that saturation in our weakly collisional, kinetic simulations is well described by the (isothermal) MHD model. At small $\Delta' a$, this agreement breaks down, because the island saturation amplitude becomes comparable to the kinetic scales (d_e, $\rho_{s,i}$). Saturation then becomes a slow, diffusive process (see Fig. 3, inset): The islands slowly expand until their width becomes $\sim d_e$. This is the lower limit to the saturation amplitude (cf. [23]); indeed, the frozen-flux condition precludes the definition of magnetic field lines at sub-d_e scales.

Electron heating.—We have established that the amount of energy converted during the evolution of the system is independent of the collisionality; we have also checked (not shown) that, for all but the smallest systems, the energy converted into electron heating is a significant fraction of the initial (magnetic) energy, reaching $\sim$60% for the largest systems. We now investigate how the energy is converted. Figure 1(b) shows the time traces of the dissipation rates for $\Delta' a = 20$ and $M = 500$. We see that dissipation is almost exclusively due to phase mixing (Landau damping), even though, *a priori*, the system was free to choose to dissipate energy via electron hyperviscosity or hyper-resistivity instead, as would *per force* be the case in any model which ignores electron kinetics [24–28]. This is a remarkable demonstration of the dominance of Landau damping over other dissipation mechanisms in weakly collisional reconnection.

The rightmost panels of Fig. 2 show that heating takes place along the separatrices of the island, not around the X point, where reconnection occurs. Inspecting Fig. 1, we also see that there is a time lag between the peaks of the reconnection and dissipation rates and that this time lag increases weakly with decreasing collisionality [Fig. 1(c)]. This is consistent with the idea that magnetic energy is not directly dissipated by the reconnection process itself [29]. Instead, the magnetic energy lost in the reconnection process is converted into ion and electron kinetic energy. Both species flow downstream predominantly along the separatrices (see streamlines of φ in the middle panels of Fig. 2). Deceleration of these flows converts kinetic energy into the free energy (or entropy) of the electrons, $\int dxdy/V \int dv_\parallel T_{0e} g_e^2/(2F_{0e})$ [8] (plotted in the top row of Fig. 4). This free energy is then transferred to higher m's via phase mixing and finally dissipated by collisions—this is the process that constitutes the energetics of Landau damping and results eventually in electron heating.

The occurrence of phase mixing is evidenced by examining the spectral maps [in the two-dimensional Fourier-Hermite ($k_\perp$, m) space] of the electron free energy and its dissipation, shown in the two top panels of Fig. 4 for $M = 500$. As time advances, indeed we see the electron free energy moving to higher values of m, corresponding to the formation of small scales in velocity space. During this process, energy dissipation occurs via the hyperdiffusive terms, acting at large values of $k_\perp$ (see the middle panel, second row of Fig. 4). At later times, large enough values of m are reached so the collisional dissipation becomes

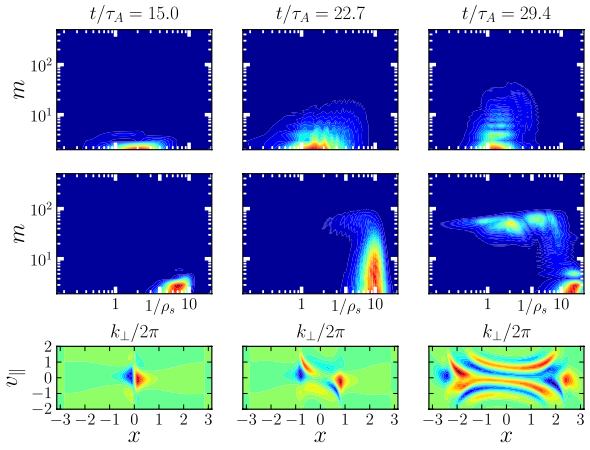

FIG. 4 (color online). Electron free energy spectrum (top row), dissipation spectrum (middle row), and a cut at $y/a = 2.3$ (see Fig. 2) of g_e (bottom row) at the early nonlinear stage (left) and at the peaks of the reconnection rate (center) and dissipation rate (right) for a run with $\Delta' a = 20$ and $M = 500$. The color scale is linear, and units are arbitrary.

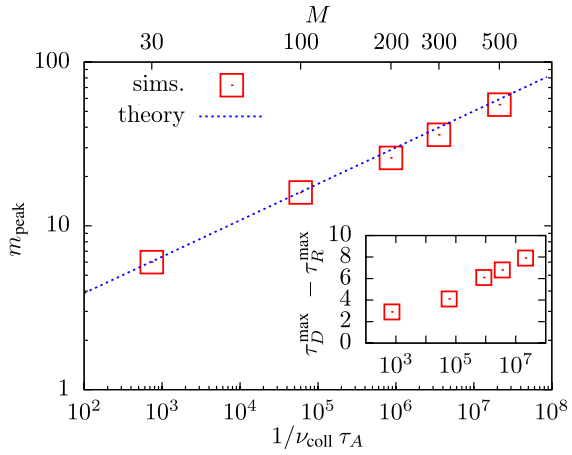

FIG. 5 (color online). Value of m at which the most energy is dissipated, $m_{\rm peak}$, as a function of collisionality, $\nu_{\rm coll}$. Inset: Time lag between the peak of the reconnection rate ($\tau_R^{\rm max}$) and the peak of the dissipation rate ($\tau_D^{\rm max}$) as a function of $\nu_{\rm coll}$.

dominant over the hyperdiffusive terms (rightmost panel, second row of Fig. 4).

To estimate the velocity-space dissipation scale, we linearize Eq. (4) for a given k_y and find that the electron free energy spectrum $E_m = |g_m|^2/2$ satisfies [8]

$$\frac{\partial E_m}{\partial t} = -|k_y|\frac{B_y}{B_z}v_{{\rm th}e}\frac{\partial}{\partial m}\sqrt{2m}E_m - 2\nu_{\rm coll}m^4E_m. \quad (5)$$

Setting $\partial E_m/\partial t = 2\gamma E_m$, we obtain

$$E_m = \frac{C(k_y)}{\sqrt{m}}\exp\left[-\left(\frac{m}{m_\gamma}\right)^{1/2} - \left(\frac{m}{m_c}\right)^{9/2}\right], \quad (6)$$

where $C(k_y)$ is some k_y-dependent constant, $m_\gamma = [k_y B_y/B_z v_{{\rm th}e}/(2\sqrt{2}\gamma)]^2$, and $m_c = [9/(2\sqrt{2})k_y B_y/B_z v_{{\rm th}e}/\nu_{\rm coll}]^{2/9}$. As is evidenced by Fig. 1(a), γ is independent of collisions, and thus so is m_γ. Therefore, while the mode is strongly growing, $m_\gamma < m_c$, and so the collisional cutoff cannot be reached. This explains why the peak of the dissipation rate must occur later than that of the reconnection rate. As reconnection proceeds into the saturation regime, $\gamma \to 0$, so, regardless of how small $\nu_{\rm coll}$ is, eventually $m_\gamma > m_c$, and, from then onwards, the Hermite spectrum cutoff is determined by m_c. In our simulations, this happens at $t \approx 26\tau_A$, roughly independent of M, because the decrease of γ is fast [see Fig. 1(a)]. The inset in Fig. 5 shows the time lag between the peaks of the reconnection and dissipation rates vs M. The logarithmic dependence is due to the fast decay of γ, and the consequent rapid increase of $m_\gamma \sim \gamma^{-2}$ to overtake m_c, thus enabling dissipation. The weak dependence of the lag on collisions implies that dissipation occurs in a finite time even for weak collisionality.

The value of $m = m_{\rm peak}$ at which most energy is dissipated is the solution of $d(\nu_{\rm coll}m^4E_m)/dm = 0$, with E_m given by Eq. (6) in the regime $m_\gamma \gg m_c$. This yields $m_{\rm peak} = (9/7)^{2/9}m_c$. This expression, evaluated for $k_y = 1$ [30], is compared in Fig. 5 with the numerical data. The remarkable agreement that is obtained shows that the electron heating we observe is the result of *linear* phase mixing due to electrons streaming along the field lines, not to the excitation of any particular wave.

The phase mixing process is illustrated by the plots of g_e in the bottom row of Fig. 4. The progressive creation of finer scales in velocity space is manifest (cf. [25,31]).

Conclusions.—This Letter presents the first investigations of electron heating caused by reconnection in strongly magnetized, weakly collisional plasmas. It is shown that electron heating is mainly due to linear phase mixing (Landau damping). We have not explored the dependence of this result on the parameters ρ_i, ρ_s, and d_e, but preliminary investigations suggest that this might be a generic feature of reconnection in such plasmas. Reconnection and electron heating are causally related but temporally and spatially disconnected: Heating happens after most flux has reconnected and along the island separatrices, not in the current sheet. Other key conclusions are (i) the maximum reconnection rate is $cE_\parallel^{\rm max} \sim 0.2 v_A B_{y,0}$, similar to the weak guide field limit, provided that the system is large enough, and (ii) the saturation amplitude in the kinetic (weakly collisional) regime is identical to that in MHD (collisional) systems [6], as long as the island is large compared to the kinetic scales. The electron inertia scale appears to provide the lower boundary on the saturation amplitude—this may be important to the understanding of electromagnetic turbulence (e.g., [32–35]), as it effectively sets the minimum fluctuation amplitude.

This work was supported by Fundação para a Ciência e Tecnologia (Ciência 2008 and Grant No. PTDC/FIS/118187/2010), by the European Communities under the Contracts of Association between EURATOM and IST and EURATOM and CCFE, and by the Leverhulme Trust Network for Magnetised Plasma Turbulence. Simulations were carried out at HPC-FF (Juelich), Jugene (PRACE), and Ranger (NCSA).

[1] E. G. Zweibel and M. Yamada, Annu. Rev. Astron. Astrophys. **47**, 291 (2009).
[2] H. P. Furth, J. Killeen, and M. N. Rosenbluth, Phys. Fluids **6**, 459 (1963).
[3] P. H. Rutherford, Phys. Fluids **16**, 1903 (1973).
[4] D. F. Escande and M. Ottaviani, Phys. Lett. A **323**, 278 (2004).
[5] F. Militello and F. Porcelli, Phys. Plasmas **11**, L13 (2004).
[6] N. F. Loureiro, S. C. Cowley, W. D. Dorland, M. G. Haines, and A. A. Schekochihin, Phys. Rev. Lett. **95**, 235003 (2005).
[7] N. F. Loureiro, R. Samtaney, A. A. Schekochihin, and D. A. Uzdensky, Phys. Plasmas **19**, 042303 (2012).
[8] A. Zocco and A. A. Schekochihin, Phys. Plasmas **18**, 102309 (2011).
[9] E. A. Frieman and L. Chen, Phys. Fluids **25**, 502 (1982).
[10] J. A. Krommes, Phys. Rep. **360**, 1 (2002).
[11] G. G. Howes, S. C. Cowley, W. Dorland, G. W. Hammett, E. Quataert, and A. A. Schekochihin, Astrophys. J. **651**, 590 (2006).
[12] I. G. Abel, G. G. Plunk, E. Wang, M. Barnes, S. C. Cowley, W. Dorland, and A. A. Schekochihin, arXiv:1209.4782.
[13] T. J. Schep, F. Pegoraro, and B. N. Kuvshinov, Phys. Plasmas **1**, 2843 (1994).
[14] N. F. Loureiro and G. W. Hammett, J. Comput. Phys. **227**, 4518 (2008).
[15] M. Ottaviani and F. Porcelli, Phys. Rev. Lett. **71**, 3802 (1993).
[16] B. Rogers and L. Zakharov, Phys. Plasmas **3**, 2411 (1996).
[17] G. Valori, D. Grasso, and H. J. de Blank, Phys. Plasmas **7**, 178 (2000).
[18] Physically, diffusive terms such as these can be related to electron finite-Larmor-radius effects. These effects, however, are ordered out in our model. Thus, their presence in our simulations can be rigorously justified only on numerical grounds.
[19] J. Birn *et al.*, J. Geophys. Res. **106**, 3715 (2001).
[20] B. N. Rogers, R. E. Denton, J. F. Drake, and M. A. Shay, Phys. Rev. Lett. **87**, 195004 (2001).
[21] B. N. Rogers, S. Kobayashi, P. Ricci, W. Dorland, J. Drake, and T. Tatsuno, Phys. Plasmas **14**, 092110 (2007).
[22] D. A. Uzdensky and R. M. Kulsrud, Phys. Plasmas **13**, 062305 (2006).
[23] R. D. Sydora, Phys. Plasmas **8**, 1929 (2001).
[24] B. N. Kuvshinov, F. Pegoraro, and T. J. Schep, Phys. Lett. A **191**, 296 (1994).
[25] D. Grasso, F. Califano, F. Pegoraro, and F. Porcelli, Phys. Rev. Lett. **86**, 5051 (2001).
[26] E. Tassi, P. J. Morrison, F. L. Waelbroeck, and D. Grasso, Plasma Phys. Controlled Fusion **50**, 085014 (2008).
[27] F. L. Waelbroeck, R. D. Hazeltine, and P. J. Morrison, Phys. Plasmas **16**, 032109 (2009).
[28] D. Del Sarto, C. Marchetto, F. Pegoraro, and F. Califano, Plasma Phys. Controlled Fusion **53**, 035008 (2011).
[29] This is why the reconnection rate should be independent of the details of the dissipation: Indeed, the same rate should be obtained even in dissipation-free models [24–28], although the energy partition would differ.
[30] We chose $k_y = 1$, because this is the characteristic scale of the energy transfer (see the top row of Fig. 4). Note, however, that $m_c \sim k_y^{2/9}$, a fairly weak dependence.
[31] T. V. Liseikina, F. Pegoraro, and E. Y. Echkina, Phys. Plasmas **11**, 3535 (2004).
[32] H. Doerk, F. Jenko, M. J. Pueschel, and D. R. Hatch, Phys. Rev. Lett. **106**, 155003 (2011).
[33] W. Guttenfelder, J. Candy, S. M. Kaye, W. M. Nevins, E. Wang, R. E. Bell, G. W. Hammett, B. P. LeBlanc, D. R. Mikkelsen, and H. Yuh, Phys. Rev. Lett. **106**, 155004 (2011).
[34] W. M. Nevins, E. Wang, and J. Candy, Phys. Rev. Lett. **106**, 065003 (2011).
[35] D. R. Hatch, M. J. Pueschel, F. Jenko, W. M. Nevins, P. W. Terry, and H. Doerk, Phys. Rev. Lett. **108**, 235002 (2012).